Chemistry of Metals and Alloys

Chem. Met. Alloys 17 (2024) 13-23
Ivan Franko National University of Lviv
http://publications.lnu.edu.ua/chemetal

The Li–Ag–In ternary system

Grygoriy DMYTRIV[1]*, Volodymyr PAVLYUK[1], Ivan TARASIUK[1], Ihor CHUMAK[2], Helmut EHRENBERG[2], Anatoliy SYNYSHYN[3], Hermann PAULY[4]

[1] *Department of Inorganic Chemistry, Ivan Franko National University of Lviv, Kyryla i Mefodiya St. 6, 79005 Lviv, Ukraine*
[2] *Institute for Applied Materials, Karlsruhe Institute of Technology, Hermann-von-Helmholtz-Platz 1, D-76344 Eggenstein-Leopoldshafen, Germany*
[3] *FRM-II, Technical University of Munich, D-85747 Garching, Germany*
[4] *Department of Materials Science, Darmstadt University of Technology, Petersenstraße 23, D-64287 Darmstadt, Germany*
* *Corresponding author. Tel.: +380-67-4398956; e-mail: grygoriy.dmytriv@lnu.edu.ua*

Received March 23, 2024; accepted July 1, 2024
https://doi.org/10.30970/cma17.0440

The interaction of the components in the Li–Ag–In system was studied in the whole concentration range based on X-ray and neutron powder diffraction. The crystal structure of the binary compound Li_3Ag was solved and refined from X-ray powder diffraction data. Three ternary compounds ($LiAg_2In$, $Li_{278}(In,Ag)_{154}$, and $Li_{2-x}Ag_{1+x}In_3$) were observed under the conditions of the experiment. The Heusler phase $LiAg_2In$ crystallizes in a $MnCu_2Al$-type structure (*Fm*-3*m*, *a* = 6.5681(5) Å). The intermetallic compound $Li_{278}(In,Ag)_{154}$ adopts a 6 × 6 × 6 superstructure of the cubic W-type (*F*-43*m*, *a* = 20.089(2) Å), and the third compound, $Li_{2-x}Ag_{1+x}In_3$, crystallizes in an own structure type (*Pmma*, *a* = 9.325(3) Å, *b* = 3.198(1) Å, *c* = 8.043(3) Å). The remarkably broad homogeneity range of the NaTl-type Zintl phase extending from LiIn into the ternary region was determined and the distribution of the atoms was obtained from refinements on X-ray and neutron diffraction data. A wide homogeneity range was also established for the binary compound Ag_3In.

Phase diagram / Intermetallics / Crystal structure / Lithium

Introduction

Investigations of the interaction between the components in ternary Li–Ag–*M* systems (*M* = *p*-element), including the construction of phase equilibria, determination of crystal structures of new compounds, and the measurement of physical properties, have been carried out intensively over the last years. However, the majority of these systems are still only partially known. The present work is part of a systematic research with the aim to investigate the constitutional properties of ternary intermetallic systems formed by lithium, transition metals and *p*-elements. These systems usually show complex phase diagrams, in which ternary compounds and solid solutions coexist. Knowledge about these systems is an essential prerequisite for further characterization of alloys potentially interesting from the practical point of view. Among the possible applications of some of these alloys, is the use as anode materials for lithium batteries.

In this paper we report results of an investigation of the interaction of the components in the Li–Ag–In system. It is a continuation of our preliminary work on ternary Zintl phases in different systems, including the Li–Ag–In system [1,2].

The next step of our investigation of the interaction of the components in this system was the determination of the homogeneity range of the wide solid solution of the Zintl phase based on the binary compound LiIn [3]. We have also published structure investigations of the ternary compounds $LiAg_2In$ [4], $Li_{278}(In,Ag)_{154}$ [5], and $Li_{2-x}Ag_{1+x}In_3$ (x = 0.05) [6].

Experimental

The samples were prepared from the following reactants: lithium (rod of 10 mm diameter, 99.9 wt.%, AlfaAesar), indium (ingots or shot, 99.999 wt.%, AlfaAesar) and silver (wire or granules 2-8 mm, 99.999 wt.%, Chempur). Appropriate amounts were

mixed and filled into unalloyed iron or tantalum crucibles under dried argon in a glove box. The iron crucibles were sealed by welding under dry argon, placed into a preheated furnace (1100°C), and heavily shaken to mix the molten reactants properly. After 10 min, the samples were rapidly cooled to room temperature by removing the crucible from the furnace. The tantalum crucibles were welded by arc melting. The reaction between the metals was carried out in an induction furnace at 1100°C. After 15 min, the samples were rapidly cooled to room temperature by removing the crucibles from the furnace. The Li-loss during sample preparation in hermetically closed crucibles can be estimated based on previous studies with detailed chemical analyses of similar systems [1,2,7].

Phase analysis of the alloys was made using powder diffraction. X-ray powder diffraction patterns were collected on a STOE STADI P diffractometer (Mo *K*α radiation) in Debye-Scherrer mode. In a glove box filled with argon, the samples were ground in an agate mortar and filled into capillaries from Hilgenberg (Germany) of 0.3 mm diameter and sealed. Intensities were recorded for different diffraction angles 2θ with steps of $\Delta 2\theta = 0.02°$. The software package WinPlotr was used for Rietveld refinements [8].

The crystal structures of the compounds were determined by means of single-crystal and powder diffraction. Single crystals for data collection were selected under dried paraffin to protect the sample against humidity, using an optical microscope. Intensity data were collected on an Xcalibur diffractometer from Oxford Diffraction, equipped with a Sapphire2 CCD detector, using the ENHANCE X-ray source option. A combined empirical absorption correction with frame scaling was applied, using the *SCALE3 ABSPACK* command in CrysalisRed [9]. The structures were solved by direct methods and refined using the SHELX-97 program package [10]. An initial parameter set was obtained from the automatic interpretation of direct methods, using SHELXS-97, and the structure models were further refined until convergence, using SHELXL-97.

For selected alloys, neutron diffraction patterns were collected on the instrument SPODI (neutron reactor FRM-II in Garching) at room temperature and 10 K with a wavelength of 1.549 Å. For these measurements, approximately 1 cm^3 of powder was ground under argon in a glove box, using an agate mortar with large diameter. Later, the powder was filled into a vanadium container with 8 mm diameter, also under argon in a glove box.

Results and discussion

Binary systems

The phase diagrams of the Li–In, Ag–In, and Li–Ag systems were not investigated here, because they have already been studied and are described in the literature [11-15]. However, some binary alloys were prepared to refine the crystal structures of particular binary compounds. Crystallographic characteristics of the binary compounds that form in the Li–In, Ag–In, and Li–Ag binary systems are presented in Table 1. Phase diagrams of the Li–In, Ag–In, Li–Ag binary systems are shown on Figs. 1-3.

Li–In. A few different variants of the phase diagram are available in the literature. An assessed phase diagram is present in ASM International Database [15] (Fig. 1). Other variants of this diagram had earlier been proposed by Thümel and Klemm [16] and Alexander *et al.* [17]. Thümel and Klemm [16] report the phases LiIn, Li_3In_2, Li_9In_4, Li_3In, Li_4In, Li_9In_2, Li_9In, and $Li_{20}In$, whereas Alexander *et al.* [17] consider the phases LiIn, Li_7In_4, Li_2In, Li_5In_2, Li_8In_3, $Li_{11}In_4$, Li_3In Li_4In, Li_6In, $Li_{12}In$, and a phase with unknown composition Li_xIn_y. The assessed diagram in ASM International Database [15] includes the phases LiIn, Li_5In_4, Li_3In_2, Li_2In Li_3In, $Li_{13}In_3$, and Li_7In. We investigated lithium-rich alloys to obtain more information about the composition and structure of the binary compounds. By X-ray single-crystal diffraction, we determined the structures of the binary compounds $Li_{22-x}In_{8+x}$ ($x = 0.1$), $Li_{11-x}In_{4+x}$ ($x = 1.05$) and $Li_{10-x}In_{2+x}$ ($x = 1.59$). Crystallographic parameters of these and other compounds confirmed by us in the Li–In system are presented in Table 1.

Li–Ag. The assessed phase diagram for the Li–Ag binary system was taken from ASM International Database [15] and is mainly based on the work by Freeth and Raynor [22] (Fig. 2). Four binary compounds were reported by these authors: β, γ_1, γ_2, and γ_3. β, γ_3, and γ_2 phases were confirmed by us by X-ray diffraction. For the γ_3 phase Noritake *et al.* [23] proposed the composition $Li_{16}Ag_9$ and the lattice parameter 9.6066 Å, which was confirmed by us in multiphase alloys. A single-phase alloy with nominal composition $Li_{75}Ag_{25}$ was prepared and the crystal structure analysis by powder diffraction showed that this compound crystallizes in the structure type BiF_3 (*Fm*-3*m*, $a = 6.5151(1)$ Å), while Freeth and Raynor [22] described this compound as cubic γ-brass Cu_5Zn_8 (*I*-43*m*, $a = 9.68$ Å). The experimental X-ray diffraction pattern, calculated profile and the difference curve after Rietveld refinement ($R_B = 5.34\%$, $R_F = 4.58\%$) are shown in Fig. 4. Refined atomic parameters for Li_3Ag are presented in Table 2. For the β phase (LiAg), the existence of a low-temperature modification was established in [24] (UPb-type structure, *I*4$_1$/*amd*, $a = 3.9605(1)$, $c = 8.2825(2)$ Å). The phase transition is very fast at the first stage, but complete transformation from CsCl cubic structure to UPb tetragonal structure occurred after 20-25 weeks.

Ag–In. The assessed phase diagram for the Li–Ag binary system was taken from ASM International Database [15] and is shown in Fig. 3. Four binary compounds, α'(Ag_3In) [25], ξ(Ag_3In) [26], γ(Ag_9In_4) [27] and $AgIn_2$ [28], and their crystal structures have been reported. Only two of them, ξ(Ag_3In) and $AgIn_2$, were confirmed by us in the Li–Ag–In system.

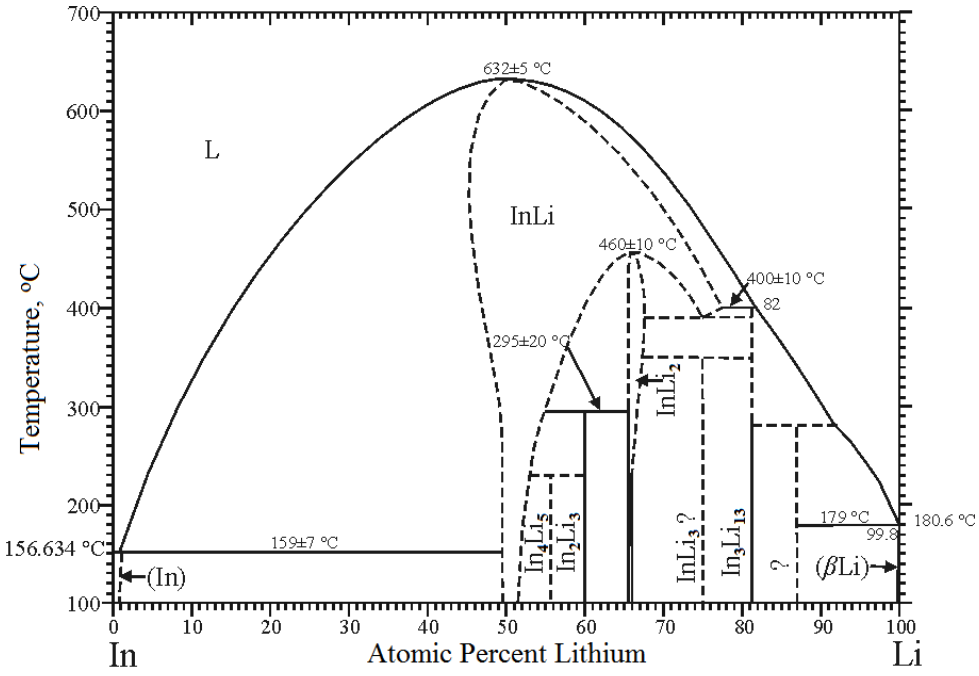

Fig. 1 Li–In binary phase diagram from ASM International Database.

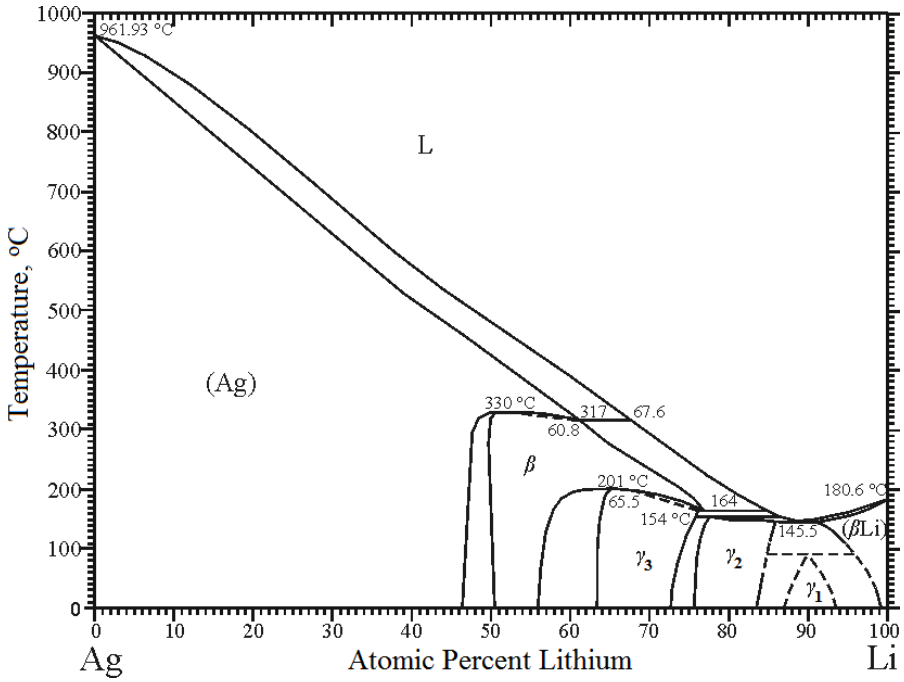

Fig. 2 Li–Ag binary phase diagram from ASM International Database.

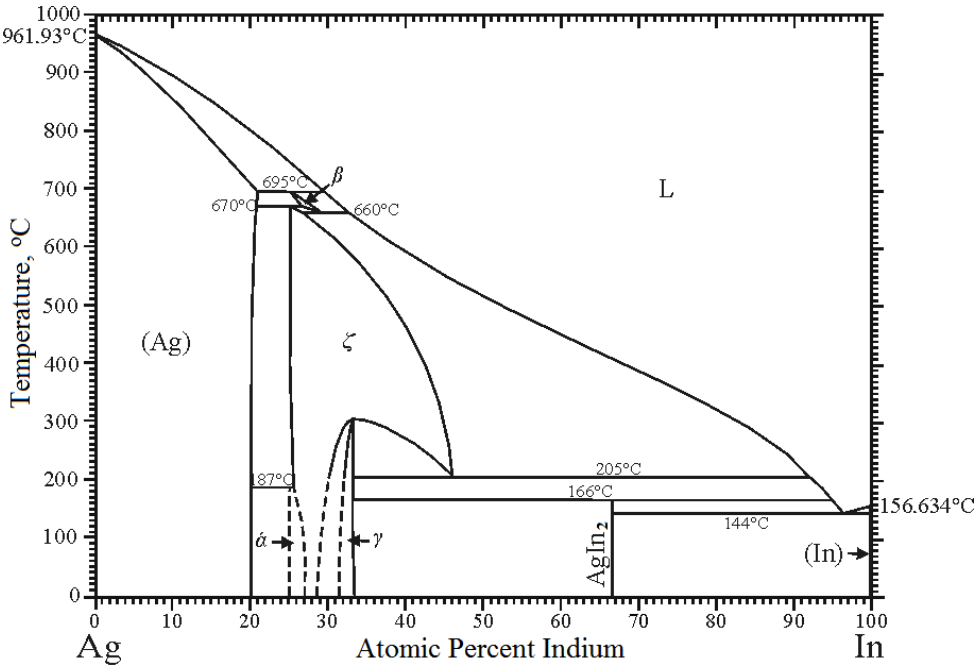

Fig. 3 Ag–In binary phase diagram from ASM International database.

Table 1 Binary compounds confirmed in the Li-Ag-In system.

Compound	Structure type	Space group	Unit-cell dimensions, Å			References
			a	*b*	*c*	
LiIn	NaTl	*Fd*-3*m*	6.792	–	–	[15,16,17,18]
Li_3In_2	Bi_2Te_3	*R*-3*m*	4.748	–	14.740	[15,16,19]
Li_2In	Li_2Ga	*Cmcm*	4.763	10.017	4.735	[15,17,20]
$Li_{22-x}In_{8+x}$ (x = 0.1)	$Li_{22-x}In_{8+x}$	*C*2/*m*	14.156(3)	4.729(1) β=105.89(1)°	8.617(2)	[21]
$Li_{11-x}In_{4+x}$ (x = 1.05)	$Li_{11-x}In_{4+x}$	*P*-3*m*1	4.7480(7)	–	14.283(3)	[21]
$Li_{10-x}In_{2+x}$ (x = 1.59)	$Li_{10-x}In_{2+x}$	*P*6/*mmm*	4.6975(7)	–	11.526(2)	[21]
$Li_{13}In_3$	$Li_{13}In_3$	*Fd*-3*m*	13.556	–	–	[15,20]
β (LiAg HT)	CsCl	*Pm*-3*m*	3.168	–	–	[22]
LiAg LT	UPb	*I*4$_1$/*amd*	3.9605(1)	–	8.2825(2)	[24]
γ_3 (Li_9Ag_4) $Li_{16}Ag_9$	Cu_9Al_4	*P*-43*m*	9.8018 9.6066	– –	– –	[22] [23]
γ_2 (Li_3Ag)	BiF_3	*Fm*-3*m*	6.5151(1)	–	–	this work
ξ (Ag_3In)	Mg	*P*6$_3$/*mmc*	2.961	–	4.778	[26]
$AgIn_2$	$CuAl_2$	*I*4/*mcm*	6.881	–	5.620	[28]

Table 2 Atomic parameters for Li_3Ag from X-ray powder diffraction (*Fm*-3*m*, a = 6.5151(1) Å).

Atom	Wyckoff position	Occupation	*x*/*a*	*y*/*b*	*z*/*c*	*B*, Å^2
Li	8*c*	1.0	¼	¼	¼	5.0
*M*1	4*a*	3.69(4)Li + 0.31(4)Ag	0	0	0	2.66(1)
*M*2	4*b*	0.32(1)Li + 3.68(1)Ag	½	½	½	2.91(2)

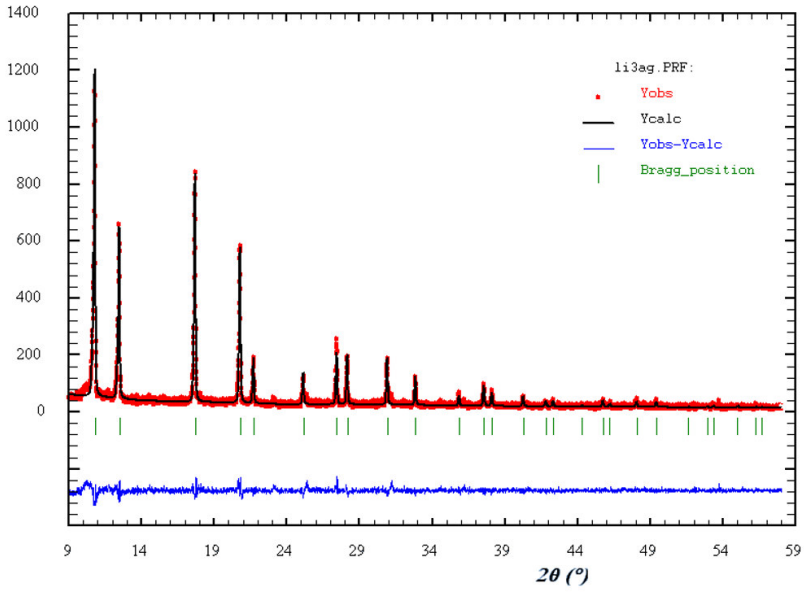

Fig. 4 Experimental X-ray diffraction pattern of Li_3Ag, calculated profile and difference after Rietveld refinement.

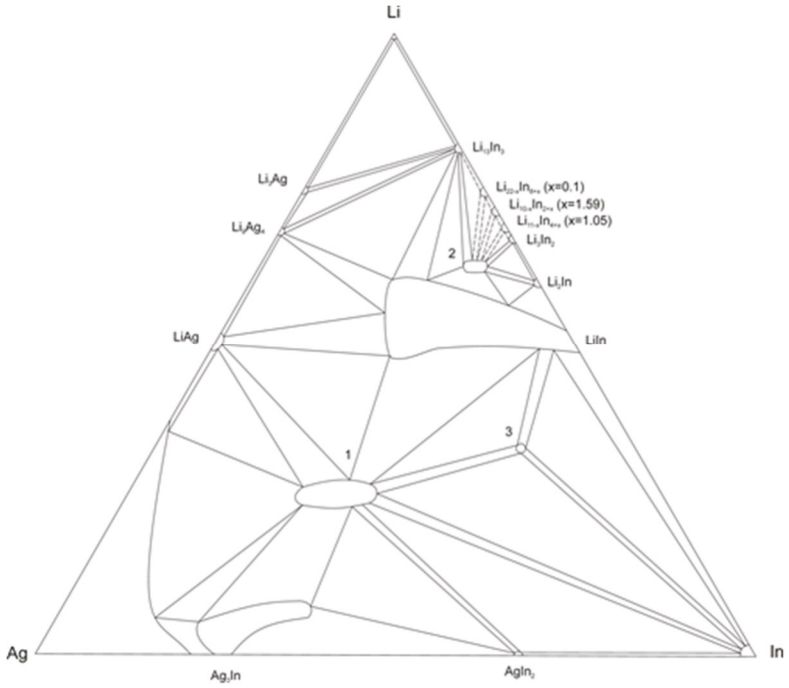

Fig. 5 Subsolidus relations in the Li–Ag–In system (as cast); 1 – $LiAg_2In$, 2 – $Li_{278}(In,Ag)_{154}$, 3 – $Li_{2-x}Ag_{1+x}In_3$ (x = 0.05).

Ternary system Li–Ag–In

The phase equilibria in the Li–Ag–In system were studied on 77 ternary as-cast alloys. The diagram of subsolidus relations in the Li–Ag–In system was constructed over the whole concentration range (Fig. 5). After annealing the alloys at 370 K, we did not observe any serious changes in the phase diagram. Chemical and phase compositions, as well as lattice parameters refined on X-ray powder diffraction data, are listed in Table 3.

The formation of two wide solid solutions on the base of binary compounds was established in the system. The largest solid solution was observed for the Zintl phase LiIn.

Table 3 Phase composition of selected alloys in the Li–Ag–In system.

Nominal alloy composition	Phase composition	Structure types	Unit-cell dimensions, Å
$Li_5Ag_{62}In_{33}$	ξ	Mg	3.0011(1) 4.7706(3)
$Li_5Ag_{66}In_{29}$	ξ	Mg	2.9744(1) 4.7813(2)
$Li_5Ag_{70}In_{25}$	ξ	Mg	2.9551(2) 4.7880(3)
$Li_5Ag_{75}In_{20}$	(Ag) + ξ	Cu + Mg	4.1441(4) + 2.9532(3) 4.790(1)
$Li_5Ag_{80}In_{15}$	(Ag)	Cu	4.1313(2)
$Li_8Ag_{70}In_{22}$	ξ + (Ag) + HP	Mg + Cu + $MnCu_2Al$	2.9512(6) 4.788(1) + 4.1532(9) + 6.594(1)
$Li_{10}Ag_{30}In_{60}$	$AgIn_2$ + HP + In	$CuAl_2$ + $MnCu_2Al$ + In	6.8806(4) 5.6081(6) + 6.4800(8) + 3.2537(1) 4.9364(3)
$Li_{10}Ag_{55}In_{35}$	ξ + $AgIn_2$	Mg + $CuAl_2$	2.9972(1) 4.7739(2) + 6.878(1) 5.616(2)
$Li_{10}Ag_{80}In_{10}$	(Ag)	Cu	4.1045(2)
$Li_{15}Ag_{57}In_{28}$	HP + ξ	$MnCu_2Al$ + Mg	6.5884(3) + 2.9782(1) 4.7756(4)
$Li_{20}Ag_{10}In_{70}$	In + $Li_{2-x}Ag_{1+x}In_3$ (x=0.05)	In + $Li_{2-x}Ag_{1+x}In_3$	3.255(1) 4.931(2) + 9.325(3) 3.198(1) 8.043(3)
$Li_{20}Ag_{50}In_{30}$	HP + ξ	$MnCu_2Al$ + Mg	6.6019(3) + 2.9994(4) 4.762(1)
$Li_{20}Ag_{60}In_{20}$	HP + (Ag)	$MnCu_2Al$ + Cu	6.5665(4) + 4.1165(3)
$Li_{24.8}Ag_{46.5}In_{28.7}$	HP	$MnCu_2Al$	6.5989(2)
$Li_{25}Ag_{25}In_{50}$	HP + In + OP	$MnCu_2Al$ + In + $Li_{2-x}Ag_{1+x}In_3$	6.6441(5) + 3.2633(2) 4.9476(6) + 9.325(3) 3.198(1) 8.043(3)
$Li_{25}Ag_{42}In_{33}$	HP	$MnCu_2Al$	6.6427(3)
$Li_{25}Ag_{50}In_{25}$	HP	$MnCu_2Al$	6.5696(3) 6.5298(5)*
$Li_{25}Ag_{70}In_5$	(Ag)	Cu	4.0755(2)
$Li_{28}Ag_{44}In_{28}$	HP	$MnCu_2Al$	6.5812(6)
$Li_{38}Ag_{31}In_{31}$	HP + ZP	$MnCu_2Al$ + NaTl	6.5705(2) + 6.6728(3)

Table 3 (continued)

$Li_{40}Ag_5In_{55}$	ZP + In + OP	NaTl + In+ $Li_{2-x}Ag_{1+x}In_3$	6.7608(2) + 3.2690(5) 4.896(3) + 9.3291(9) 3.1988(4) 8.0311(8)
$Li_{44}Ag_{15.5}In_{40.5}$	ZP + HP	NaTl + $MnCu_2Al$	6.6162(1) + 6.73482(8)
$Li_{47}Ag_{26.5}In_{26.5}$	ZP	NaTl	6.5796(1) 6.5453(4)[a]
$Li_{48.5}Ag_{13.25}In_{38.25}$	ZP	NaTl	6.6862(5) 6.6587(8)[a]
$Li_{50}Ag_{25}In_{25}$	ZP	NaTl	6.57971(3)
$Li_{50}Ag_{40}In_{10}$	LiAg + ZP	UPb + NaTl	4.041(1) 8.158(3) + 6.556(2)
$Li_{56}Ag_{9.5}In_{34.5}$	ZP	NaTl	6.6756(1)
$Li_{60}Ag_{20}In_{20}$	ZP	NaTl	6.5746(3)
$Li_{65}Ag_5In_{30}$	BC + Li_2In	$Li_{278}(Ag,In)_{154}$ + Li_2Ga	20.0498(5) 19.919(2)[a] + 4.7485(5) 10.045(1) 4.7328(5)
$Li_{65}Ag_7In_{28}$	BC	$Li_{278}(Ag,In)_{154}$	20.0191(7)
$Li_{65}Ag_{30}In_5$	γ_3 + ZP	Cu_9Al_4 + NaTl	9.5938(2) + 6.6271(5)
$Li_{70}Ag_{10}In_{20}$	$Li_{13}In_3$+ ZP	$Li_{13}In_3$ + NaTl	13.2172(5) + 6.6205(4)
$Li_{70}Ag_{20}In_{10}$	γ_3 + $Li_{13}In_3$+ ZP	Cu_9Al_4 + $Li_{13}In_3$ + NaTl	9.5947(2) + 13.2885(4) + 6.6388(3)
$Li_{80}Ag_{10}In_{10}$	$Li_{13}In_3$ + γ_2	$Li_{13}In_3$ + BiF_3	13.3932(1) + 6.5332(1)

HP – Heusler phase [4]
ZP – Zintl phase [3]
BC – "big cell compound" with cubic structure [5]
OP – phase with orthorhombic structure [6]
[a] – neutron data

We investigated this solid solution by X-ray powder diffraction along 4 isoconcentrates. Along all of them a wide solid solution was established: Li_xIn_{1-x} with $0.47 \le x \le 0.55$ [29,30], $Li_{0.5}(Ag_{1-x}In_x)_{0.5}$ with $0.47 \le x \le 1.00$ [2,31], $Li_x(Ag_{0.5}In_{0.5})_{1-x}$ with $0.44 \le x \le 0.62$ [3] and $Li_x(Ag_{\approx 0.25}In_{\approx 0.75})_{1-x}$ with $0.49 \le x \le 0.58$ [3]. The color of the investigated Zintl phase correlates with the valence electron concentration (VEC), as already established for the quasibinary section $Li_{0.5}(In_xAg_{1-x})_{0.5}$ with $0.47 \le x \le 1.00$, so that with decreasing VEC the color changes from gray, *via* reddish, to bright yellow.

The hexagonal compound Ag_3In (ξ) deeply extends into the ternary field, dissolving up to 10 at.% Li. The mechanism of formation of this solid solution is complex, since it involves not only incorporation of Li into the binary compound Ag_3In (for the maximal Li content the lattice parameters increase to $a = 3.2537(1)$ Å and $c = 4.9364(3)$ Å), but also substitution of Ag atoms for In atoms. The lattice parameters along the isoconcentrate 5 at.% Li change from $a = 3.0011(1)$ Å, $c = 4.7706(3)$ Å for 33 at.% In to $a = 2.9532(3)$ Å, $c = 4.790(1)$ Å for 22 at.% In (Fig. 6).

The other binary compounds in the boundary systems do not dissolve significant amounts of the third component. The homogeneity region of the solid solution on the base of silver (Ag) was estimated from alloys with compositions $Li_5Ag_{80}In_{15}$, $Li_{10}Ag_{80}In_{10}$, and $Li_{25}Ag_{70}In_5$. The lattice parameter in this area changes from $a = 4.1313(2)$ Å to $a = 4.0755(2)$ Å.

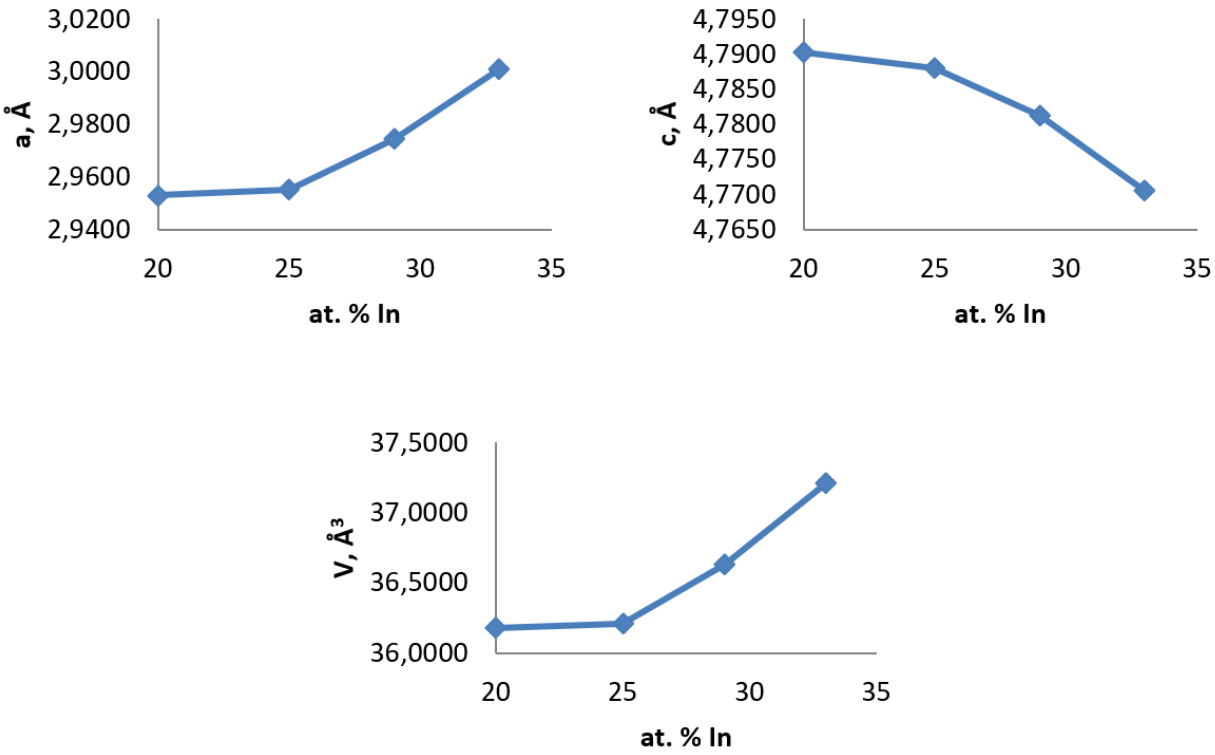

Fig. 6 Unit-cell dimensions and volume of the solid solution based on the binary compound Ag_3In along the isoconcentrate 5 at.% Li.

Three ternary phases were found in the Li–Ag–In system. $LiAg_2In$ [4] crystallizes in a $MnCu_2Al$-type structure (*Fm*-3*m*, Heusler phase). This compound has a wide homogeneity range, mainly along the isoconcentrate 25 at.% Li, where the unit-cell dimensions change from $a = 6.5696(3)$ Å to $a = 6.6427(3)$ Å with increasing In content from 25 to 33 at.%. The second compound, $Li_{278}(In,Ag)_{154}$ [5], crystallizes in a $n \times n \times n$ superstructure of the cubic W-type with $n = 6$ (space group *F*-43*m*). This phase exists in a much smaller homogeneity region, within which the lattice parameters change from $a = 20.0191(7)$ Å to $a = 20.0615(4)$ Å. The third intermetallic compound, $Li_{2-x}Ag_{1+x}In_3$ ($x = 0.05$) [6], crystallizes in an own structure type (space group *Pmma* ($a = 9.325(3)$ Å, $b = 3.198(1)$ Å, $c = 8.043(3)$ Å) and exists in a narrow homogeneity range.

Experimental X-ray and neutron diffraction patterns of some of the ternary alloys from the Li–Ag–In system, calculated profiles and their difference curve after Rietveld refinement, are shown in Fig. 7. The main purpose of the neutron diffraction investigation was to establish the real occupation in the statistical mixtures Li+Ag and Li+In in the structures of alloys belonging to the wide solid solution based on the Zintl phase LiIn, situated on the borderline of the two quasibinary sections $Li_x(Ag_{0.5}In_{0.5})_{1-x}$ and $Li_x(Ag_{\sim 0.25}In_{\sim 0.75})_{1-x}$. The atomic parameters for the alloy with composition $Li_{47.0}Ag_{26.5}In_{26.5}$ refined to $R_B = 2.80\%$ and $R_F = 2.25\%$ (XRD data) and $R_B = 6.11\%$ and $R_F = 5.93\%$ (neutron data) and are listed in Table 4. The atomic parameters (Table 4) of the alloy with composition $Li_{48.5}Ag_{13.25}In_{38.25}$ were refined to $R_B = 5.84\%$ and $R_F = 7.21\%$ (XRD data) and $R_B = 5.89\%$, $R_F = 4.14\%$ (neutron data).

Summary

Three ternary compounds were observed in the Li–Ag–In system. The intermetallic compound $LiAg_2In$ crystallizes in a $MnCu_2Al$-type structure (*Fm*-3*m*, Heusler phase, $a = 6.5681(5)$ Å, $Li_{278}(In,Ag)_{154}$ in a cubic $6 \times 6 \times 6$ superstructure of the W-type (*F*-43*m*, $a = 20.089(2)$ Å), and $Li_{2-x}Ag_{1+x}In_3$ forms an own structure type (*Pmma*, $a = 9.325(3)$ Å, $b = 3.198(1)$ Å, $c = 8.043(3)$ Å for $x = 0.05$). The remarkably broad homogeneity range of the Zintl phase extending from LiIn into the ternary Li–In–Ag system was determined, and the distribution of the atoms studied on X-ray and neutron diffraction data. A wide homogeneity range was also established for the binary compound Ag_3In.

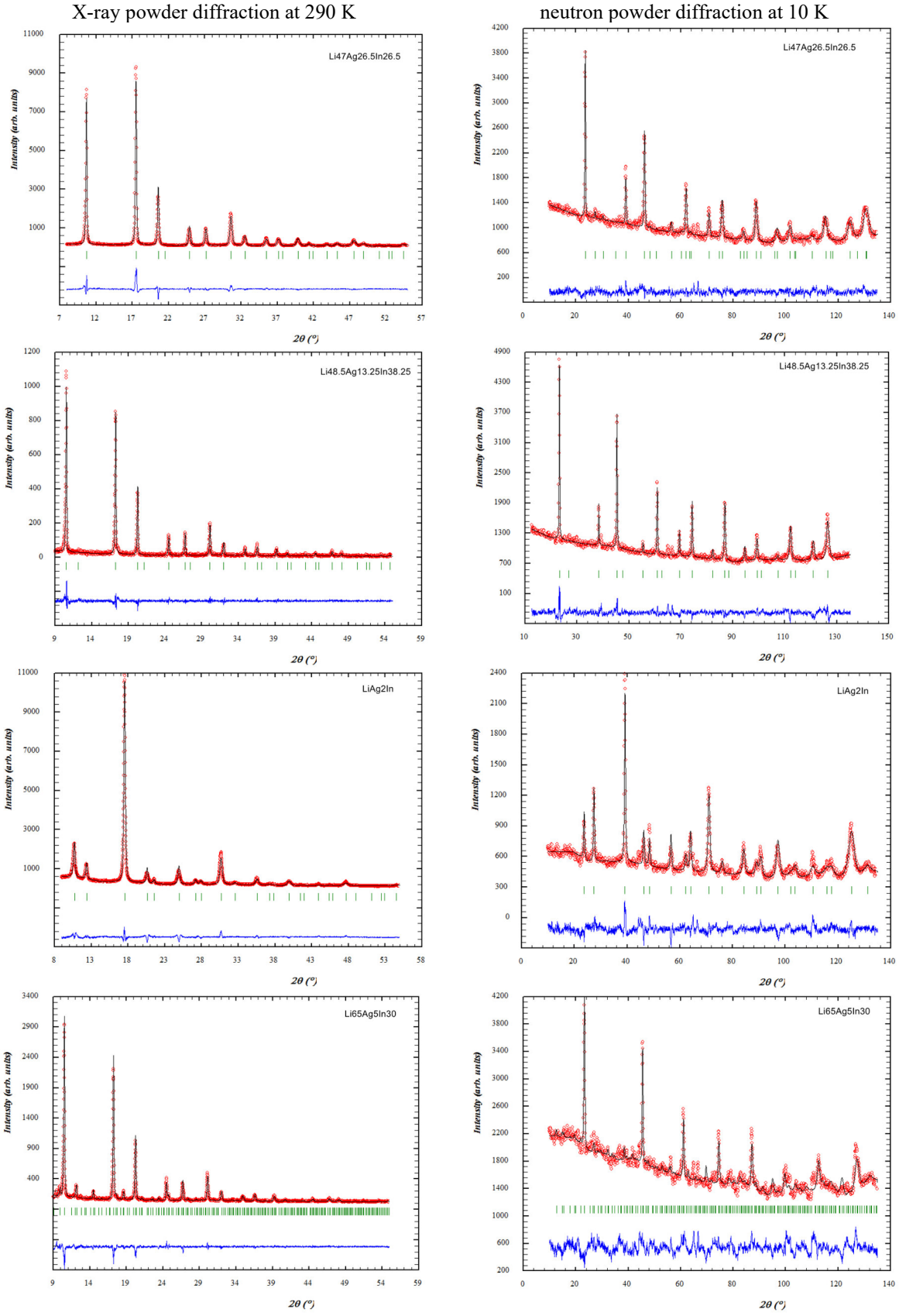

Fig. 7 Experimental X-ray and neutron diffraction patterns of the alloys $Li_{47.0}Ag_{26.5}In_{26.5}$, $Li_{48.5}Ag_{13.25}In_{38.25}$, $Li_{25}Ag_{50}In_{25}$, and $Li_{65}Ag_5In_{30}$, calculated profiles and their difference curve after Rietveld refinement.

Table 4 Refined atomic parameters for $Li_{47.0}Ag_{26.5}In_{26.5}$ and $Li_{48.5}Ag_{13.25}In_{38.25}$.

Atom	Wyckoff position	Occupation		*x/a*	*y/b*	*z/c*	*B*, Å^2	
		XRD data	Neutron data				XRD	Neutron
$Li_{47.0}Ag_{26.5}In_{26.5}$								
Ag1	4*a*	1.000	1.000	0	0	0	1.55	0.76
In1	4*c*	1.000	1.000	¼	¼	¼	1.78	1.04
M1	4*b*	0.936(6) Li 0.064(6) Ag	0.937(9) Li 0.063(9) Ag	½	½	½	2.21	2.12
M2	4*d*	0.937(7) Li 0.063(7) Ag	0.94(1) Li 0.06(1) In	¾	¾	¾	2.43	2.12
$Li_{48.5}Ag_{13.25}In_{38.25}$								
In1	4*a*	1.000		0	0	0	1.12	0.81
M1	4*c*	0.529(8) In 0.471(8) Ag	0.54(1) In 0.46(1) Ag	¼	¼	¼	1.14 1.14	0.92 0.92
Li1	4*b*	1.000	1.000	½	½	½	2.06	2.87
M2	4*d*	0.95(1) Li 0.05(1) Ag	0.94(2) Li 0.06(2) Ag	¾	¾	¾	1.12 1.12	1.04 1.04

Acknowledgements

This work was carried out under grants of the Ministry of Education and Science of Ukraine No. 0124U000989, National Research Foundation of Ukraine No. 2022.01/0064 and Simons Foundation No. 1290588.

References

[1] H. Pauly, *PhD Thesis*, Darmstadt University of Technology, 1966.
[2] H. Pauly, A. Weiss, H. Witte, *Z. Metallkd.* 59 (1968) 47-58.
[3] G. Dmytriv, H. Pauly, H. Ehrenberg, V. Pavlyuk, E. Vollmar, *J. Solid State Chem.* 178 (2005) 2825-2831.
[4] V. Pavlyuk, G. Dmytriv, I. Chumak, H. Ehrenberg, H. Pauly, *J. Solid State Chem.* 178 (2005) 3303-3307.
[5] V. Pavlyuk, G. Dmytriv, I. Tarasiuk, H. Ehrenberg, H. Pauly, *Intermetallics* 15 (2007) 1409-1415.
[6] I. Chumak, V. Pavlyuk, G. Dmytriv, H. Pauly, H. Ehrenberg, *J. Solid State Chem.* 197 (2013) 248-253.
[7] H. Pauly, *Diploma Thesis*, Darmstadt University of Technology, 1963.
[8] T. Roisnel, J. Rodriguez-Carvajal, *Mater. Sci. Forum* 378-381 (2001) 118-123.
[9] CrysalisRed, *CCD data reduction GUI*, Version 1.171.26, Oxford Diffraction Poland Sp., 2005.
[10] G.M. Sheldrick, SHELXL-97, *Program for Crystal Structure Refinement.* University of Göttingen, Germany, 1997.
[11] G. Effenberg, F. Aldinger, O. Bodak (eds.) and V.V. Pavlyuk (assoc. ed.), *Ternary Alloys (+ Binary + Quaternary Systems. Evaluated Constitutional Data, Phase Diagrams, Crystal Structures and Applications of Lithium Alloy Systems),* VCH, D-69496 Weinheim, Germany. Vol. 14, 1995, 458 p.
[12] G. Effenberg, F. Aldinger, O. Bodak (eds.) and V.V. Pavlyuk (assoc. ed.), *Ternary Alloys (+Binary + Quaternary Systems. Evaluated Constitutional Data, Phase Diagrams, Crystal Structures and Applications of Lithium Alloy Systems).* VCH, D-69496 Weinheim, Germany. Vol. 15, 1995, 448 p.
[13] T.B. Massalski, in: *Binary Alloys Phase Diagrams*, Vol. 122, American Society for Metals, Metals Park, Ohio, 1986, 2223 p.
[14] P. Villars, L.D. Calvert (eds.), *Pearson's Handbook of Crystallographic Data for Intermetallic Phases*, American Society for Metals, Ohio, 1983, 3258 p.
[15] *Binary Alloy Phase Diagram Resources*, ASM International.
[16] R. Thümel, W. Klemm, *Z. Anorg. Allg. Chem*. 376 (1970) 44-63.
[17] W.A. Alexander, L.D. Calvert, R.H. Gamble, K. Schinzel, *Can. J. Chem*. 54 (1976) 1052-1060.
[18] E. Zintl, G. Brauer, *Z. Phys. Chem*. 20 (1933) 245-271.
[19] J. Stöhr, H. Schäfer, *Z. Naturforsch. B* 34 (1979) 653-656.
[20] J. Stöhr, W. Müller, H. Schäfer, *Z. Naturforsch. B* 33 (1978) 1434-1437.
[21] I. Chumak, V. Pavlyuk, H. Ehrenberg, *Eur. J. Inorg. Chem.* 12 (2014) 2053-2064.
[22] W.E. Freeth, G.V. Raynor, *J. Inst. Met*. 82 (1953-1954) 569-574.
[23] T. Noritake, M. Aoki, S. Towata, T. Takeuchi, U. Mizutani, *Acta Crystallogr. B* 63 (2007) 726-734.
[24] V. Pavlyuk, G. Dmytriv, I. Tarasiuk, I. Chumak, H. Pauly, H. Ehrenberg, *Solid State Sci.* 12 (2010) 274-280.

[25] A.N. Campbell, R. Wagemann, R.B. Ferguson, *Can. J. Chem*. 48 (1970) 1703-1715.
[26] D.P. Morris, I. Williams, *Acta Crystallogr*. 14 (1961) 74.
[27] J.K. Brandon, R. Brezard, W.B. Pearson, D.J.N. Tozer, *Acta Crystallogr*. *B* 33 (1977) 527-537.
[28] E.E. Havinga, H. Damsma, P. Hokkeling, *J. Less-Common Met*. 27 (1972) 169-186.
[29] K. Kuriyama, *J. Cryst. Growth* 23 (1974) 160-162.
[30] T.S. Huang, J.O. Brittain, *Mater. Sci. Eng*. 93 (1987) 83-92.
[31] H. Pauly, A. Weiss, H. Witte. *Z. Metallkd*. 59 (1968) 554-558.